Geophys. J. Int. (1994) **117**, 577–590

The nature and cause of polarization anomalies of surface waves crossing northern and central Eurasia

Anatoli L. Levshin, Michael H. Ritzwoller and Ludmila I. Ratnikova
Department of Physics, University of Colorado, Campus Box 583, Boulder, CO 80309–0583, USA

Accepted 1993 September 14. Received 1993 August 23; in original form 1992 November 24

SUMMARY

Results of a pilot experiment preliminary to a systematic study of surface-wave polarization across Eurasia are presented. Long-period fundamental Rayleigh and Love waves recorded by the broad-band seismic stations KIV (Kislovodsk) and OBN (Obninsk) of the IRIS/IDA network deployed in the Former Soviet Union (FSU) were analysed from 14 events to the north-east, east and south-east of these stations in search of particle-motion anomalies using a technique called Frequency–Time Polarization Analysis (FTPAN). All anomalies indicate deviations of wave-propagation paths to the north relative to the great circle paths. Polarization anomalies at OBN are uniformly small (<5°). Significant frequency-dependent polarization anomalies (5°–20°) are found for Rayleigh and Love waves arriving at KIV from teleseismic events at a wide range of backazimuths (26°–103°). Polarization measurements are repeatable (both for a number of nearly degenerate events and for reciprocal paths) and vary smoothly and continuously as epicentral location is moved. Consequently, such measurements are robust and can provide useful structural information. The systematics of the frequency dependence of the polarization anomalies as epicentral position is moved from north to south display sensitivity to structures at a number of length-scales.

Results from synthetic experiments using coupled normal-mode and Gaussian-beam synthetics reveal that: (1) recently constructed long-wavelength aspherical models produce polarization anomalies that are significantly smaller (<5° at KIV) but of the same sign (negative) as the observed anomalies, and (2) the frequency dependence of the observed anomalies must result from a combination of structures of differing wavelengths, with scale-lengths ranging from regional to global. Thus, polarization measurements provide new information about currently unmodelled structures. A model that fits the polarization anomalies observed at KIV includes a regional-scale low-velocity feature near to KIV in order to fit the large-magnitude, short-period polarization anomalies and a smaller magnitude, continent-scale increase in upper mantle velocities and/or the reduction of crustal thickness from south to north in central Eurasia in order to fit the broad-band, longer period anomalies. The small-scale, low-velocity feature is a model of the sedimentary basin of the sub-Caspian depression.

We conclude that measurements of polarization anomalies can be obtained accurately, that they are reproducible, that they contain currently unmodelled information, and that they should prove to be useful in combination with velocity and amplitude information in future tomographic inversions, especially to help focus global-scale models to regional wavelengths.

Key words: Eurasia, lateral heterogeneity, polarization, surface waves, synthetic seismograms.

1 INTRODUCTION

Surface-wave tomography has now become a standard means for studying the lateral heterogeneity of the Earth's crust and upper mantle (e.g. Leveque & Cara 1983, 1985; Woodhouse & Dziewonski 1984; Tanimoto & Anderson 1985; Nataf, Nakanishi & Anderson 1986; Nolet 1987; Cara & Leveque 1988; Gee & Jordan 1988; Levshin *et al.* 1989; Smith & Masters 1989; Montagner & Tanimoto 1990). However, there are some basic limitations of the classical techniques which should be understood and overcome if global models are to be focused accurately from global (>2000 km) to regional (~1000 km) wavelengths. Classical tomography is usually based on the assumption that waves propagate along great circles between the source and receiver (exceptions include Wong 1989, and Durek, Ritzwoller & Woodhouse 1993). The same assumption is implicitly present in approaches using waveform inversion, since only phase distortions due to lateral heterogeneity are usually taken into account. Since velocity perturbations along the wave path through different tectonic regimes may be severe, surface-wave 'path wander' can be appreciable, and the great-circle assumption is not justified if one is interested in subglobal scale wavelengths.

One way to estimate the strength of deviations of waves from great circle paths is to use array observations (e.g. Bungum & Capon 1974; Levshin & Berteussen 1979; Berteussen, Levshin & Ratnikova 1983; Lander & Levshin 1982). Several authors have observed azimuthal deviations of surface wavefronts across arrays from those predicted by source–receiver geometries. Owing to the bandwidth limitations of the instruments used and the limited aperture of the arrays (100 km or less), these observations covered only the middle part of the surface-wave spectrum (periods from 10 to 40 s) for which waves propagate mainly in the crust and do not penetrate into the mantle. The observed anomalies were mainly attributed to refraction at continental margins. Later arrivals in the surface-wave coda have also been found with azimuths of approach significantly different from those of the main wavetrains, diagnostic of complicated multipathing due to reflection and refraction of surface waves in the Earth's crust.

Another way to estimate surface-wave azimuthal 'wandering' is to study particle motion or polarization (e.g. Lander & Levshin 1982; Vidale 1986; Lerner-Lam & Park 1989). It is believed from asymptotic theories describing surface-wave propagation in inhomogeneous media with smooth lateral variations (e.g. Woodhouse 1974; Babich & Chikhachev 1975; Babich, Chikhachev & Yanovskaya 1979; Yomogida & Aki 1985; Woodhouse & Wong 1986; Levshin 1985; Levshin *et al.* 1989) that particle motion on an aspherical earth should approximate the features of particle motion in media with purely depth-dependent properties. The difference is that the ray geometry on an aspherical earth is determined by the frequency-dependent phase-velocity distribution which produces a frequency-dependent rotation of the local ray basis functions at the receiver. By determining the particle motion as a function of period, the orientation of the ray basis as a function of period can be determined, which can provide additional parameters for tomographic inversions. These additional parameters (wave inclination, azimuth, amplitude) could then be added to group traveltime measurements to help to focus models otherwise distorted by unmodelled path wander. Techniques similar to those developed by Hu & Menke (1992) for body-wave inversions could then be applied.

The accuracy of polarization measurements at teleseismic distances is limited by several factors: (1) surface waves with very short periods (say less than 15–20 s) are disturbed by local small-scale effects, scattering and multipathing; (2) waves with very long periods (say more than 200–300 s) are generated only by very large events which are few in number; and (3) waves whose frequency content and group traveltimes are similar in a given time interval (e.g. Rayleigh and Love waves in continental regions with periods between 30–50 s) may interfere strongly and complicate polarization measurements (Levshin, Ratnikova & Berger 1992; Pollitz & Hennet 1993). The purpose of this study is to demonstrate that if these problems are understood and accounted for carefully, then polarization measurements can be carried out quite accurately and produce reliable, consistent and reproducible results.

For these purposes, we use a technique called the Frequency–Time Polarization Analysis (FTPAN) developed in its main features by A. Lander (Levshin *et al.* 1989) and applied previously, after some modifications, to the analysis of NARS-Iberia records by Paulssen *et al.* (1990), and to IRIS/IDA-FSU records by Levshin *et al.* (1992). The existence of strong-particle-motion anomalies on KIV records of surface waves from several events in the Western Pacific was shown by Levshin *et al.* (1992). No significant anomalies for paths from events to the South, North and West from KIV were found. The present study covers a wider range of azimuths of approach from north-east and east, considers more events than the study of Levshin *et al.* (1992), and analyses the results of forward-modelling studies concerning the source regions of the observed polarization anomalies. As we will show, polarization measurements differ appreciably from those predicted in synthetic experiments using global aspherical models, but can be reproduced from realistic regional models of the Central Eurasian lithosphere. This indicates the existence of significant unmodelled structure in Central Eurasia to which polarization studies are sensitive. Such results can be used to provide additional information in future tomographic studies of Eurasian deep structure.

Data from two IRIS/IDA stations deployed in Russia, KIV (Kislovodsk) and OBN (Obninsk), were selected for the present study. The general features of IRIS/IDA stations are described by Given (1990). Although these stations are relatively close to one another (~1300 km), they are in different tectonic regimes and, as Fig. 1 shows, the strikes of the paths of the waves arriving at each station relative to the major tectonic provinces of Eurasia differ appreciably. KIV is situated on the northern slope of the main Caucasus range, several dozens of km from Elbrus—the highest mountain in Europe. The Sciphean platform is to the north of KIV, the Black Sea and sub-Caspian depressions are, respectively, to the west and north-east, the Dnepro–Donetski graben is to the north-west. Wave paths from the events considered here cross one or several of these tectonic features. OBN is located in the middle of the Russian Platform in a simple tectonic environment and wave paths should be relatively

Figure 1. Locations of stations, events, and the great-circles linking them.

unaffected by regional-scale heterogeneities. As we will show, polarization anomalies tend to be much larger at KIV than at OBN, and OBN can be considered to be a control station.

2 DATA

Only records from events situated in and around Eurasia with strong long-period surface waves not contaminated by microseisms or internal noise were chosen for analysis, with the best results obtained from events with surface-wave magnitudes, M_s, greater than 6.5. Reliable instrument responses at KIV and OBN are known from 1989 April (H. Given, private communication, 1992), and we used records obtained from this time until 1992 January. The list of selected events together with corresponding values of station-to-epicentre backazimuths (measured at the station from the north to the epicentre) and epicentral distances is given in Table 1. Selected events are situated in a range of backazimuths from 26° to 103°, with the exception of a single event in Ethiopia, and at epicentral distances ranging from 3500 to 9000 km. Several records of the GSN station in Matsushiro (MAJO), Japan, and of the GEOSCOPE station at Inuyama (INU), Japan, for three events from 1991 and 1992 (Table 1) in the Caucasus were also processed for comparison of azimuthal anomalies observed along 'reciprocal' paths from the Caucasus to the Western Pacific.

3 DATA PROCESSING

The technique for data processing using FTPAN is described in detail in Levshin *et al.* (1989). The main output of the FTPAN method is diagrams of 'azimuthal deviations' for Rayleigh and Love waves in the frequency–time domain. For Rayleigh waves, this represents the angular difference between the strike of the plane of the quasi-elliptical particle motion and the azimuth of the station–epicentre great circle. For Love waves, this represents the angular difference between the strike of the direction orthogonal to the quasi-linear particle motion and the same great-circle azimuth. Additional, regularly utilized output are the energy of the analysed signals, their 'quality' (i.e. closeness to the considered type of particle motion, Rayleigh or Love) and other parameters related to polarization, such as the inclination of the particle orbit to vertical for Rayleigh waves and angle of near-linear particle motion trajectory with the horizon for Love waves. Only those parts of the frequency–time diagrams with the 'quality' above a selected threshold are chosen for further consideration. All the events listed in Table 1 meet quality standards, which means we believe that the reported measurements are accurate at least to a few degrees.

To estimate quantitative information we apply several techniques. One extracts the values of a measured quantity along a group-velocity curve obtained from a single-

Table 1. (a) Event locations and azimuthal deviations at station KIV. The azimuthal deviations are reported for Rayleigh and Love waves at three periods: 60 s, 100 s, and 150 s. A dash indicates that an accurate measurement could not be made. For example, (—, −10, −11) for the Luzon event indicates Rayleigh wave azimuthal anomalies −10° and −11° at 100 s and 150 s periods, respectively, with no accurate measurement at 60 s. Also, −17°, −12° and −10° deviations were oberved at 60 s, 100 s, and 150 s periods, respectively, for Love waves. (b) Same as (a), but for the station OBN. (c) Same as (a), but for the three Caucasus events observed at the GSN station MAJO. (d) Same as (c), but for the GEOSCOPE station INU.

(a)

Date m/d/y	Region	Latitude degrees	Longitude degrees	M_s	Range km	Azimuth degrees	Azimuthal Deviation T=60s, T=100s, T=150s RAYLEIGH	LOVE
03/08/91	Koryakia, Siberia	60.90	167.02	6.6	7345	26	-17, -12, -1	-, -, -
04/11/89	Kamchatka	49.48	159.18	6.5	7963	36	-13, -9, -7	-, -, -
12/13/91	Kuril Is.	45.58	151.63	6.5	7871	45	-,-13,-11	-, -, -
12/13/91	Kuril Is.	45.55	151.72	6.2	7879	45	-,-12,-11	-, -, -
12/13/91	Kuril Is.	45.43	151.30	5.8	7865	45	-,-12,-11	-, -, -
12/19/91	Kuril Is.	45.17	151.30	6.6	7879	45	-16,-12,-13	-, -, -
12/22/91	Kuril Is.	45.48	151.05	7.4	7846	45	-,-11,-10	-, -, -
09/23/90	S. Honshu	33.64	138.64	6.5	7960	61	-, -, -	-10, -6, -
09/23/90	S. Honshu	33.64	138.64	6.5	7960	61	-, -, -	-10, -6, -8
09/03/91	S. Honshu	33.64	138.78	6.4	7718	60	-, -, -	-10, -6, -
07/16/90	Luzon, Philippines	15.68	121.17	7.8	7896	86	-,-10,-11	-17,-12,-10
06/14/90	Panay, Philippines	11.33	122.17	7.0	8300	89	-, -, -	-12,-11,-11
04/18/90	Minahasa, Sulawesi	1.16	122.84	7.4	9130	96	-, -, -	-15,-11,-10
10/19/91	N. India	30.74	78.79	7.1	3484	103	-, -, -	-,-16,-17

(b)

Date m/d/y	Region	Latitude degrees	Longitude degrees	M_s	Range km	Azimuth degrees	Azimuthal Deviation T=60s T=100s T=150s RAYLEIGH	LOVE
03/08/91	Koryakia, Siberia	60.90	167.02	6.6	6433	26	-2, -2, -2	-, -, -
11/06/90	Komandorsky Is.	53.47	169.93	7.0	7232	29	0, 3, 3	-3, -1, -1
04/11/89	Kamchatka	49.48	159.18	6.5	7246	37	0, 6, 3	-, -, -
12/13/91	Kuril Is.	45.58	151.63	6.5	7294	44	-, -5, 2	-, -, -
12/19/91	Kuril Is.	45.17	151.30	6.6	7312	45	-, -7, 2	-, -, -
11/26/91	Hokkaido	42.02	142.55	-	7181	52	-, -, -	-, 2, 1
11/01/89	E. Honshu	39.80	142.84	7.3	7393	54	-, -, -	0, 1, 1
02/20/90	S. Honshu	34.69	139.35	6.4	7661	59	-, -, -	0, -2, -2
12/30/89	Bismark Sea	-3.43	146.13	6.6	11555	75	-, -, -	-4, -1, -2
08/21/89	Taiwan	24.09	122.50	6.2	7592	79	-, -, -	-, 2, -
12/15/89	Mindanao, Philippines	8.39	126.78	7.4	9261	85	-, -, -	0, 0, -
12/20/89	Mindanao, Philippines	8.13	126.88	-	9291	85	-, -, -	-2, 0, -
07/16/90	Luzon, Philippines	15.68	121.17	7.8	8250	85	-, -, -	-3, 0, 1
07/17/90	Luzon, Philippines	16.41	121.02	6.6	8176	85	-, 0, 3	-, -, -
08/21/89	Ethiopia	11.87	41.84	6.2	4819	172	-, -, -	-2, -1, -

(c)

Date m/d/y	Region	Latitude degrees	Longitude degrees	M_s	Range km	Azimuth degrees	Azimuthal Deviation T=60s T=100s T=150s RAYLEIGH	LOVE
04/29/91	W. Caucasus	42.49	43.65	7.0	7714	308	6, 14, -	8, 10, 7
06/15/91	W. Caucasus	42.44	43.99	6.1	7693	308	7, 14, -	-, -, 9
10/23/92	E. Caucasus	42.50	45.07	6.5	7613	307	-, -, -	8, 9, 8

(d)

Date m/d/y	Region	Latitude degrees	Longitude degrees	M_s	Range km	Azimuth degrees	Azimuthal Deviation T=60s T=100s T=150s RAYLEIGH	LOVE
04/29/91	W. Caucasus	42.49	43.65	7.0	7711	308	6, -, -	8, 9, 8
06/15/91	W. Caucasus	42.44	43.99	6.1	7690	308	-, -, -	-, -, 9
10/23/92	E. Caucasus	42.50	45.07	6.5	7609	307	-, -, -	6, 8, 8

component record by the frequency–time analysis. The vertical component record is used for Rayleigh waves and the transverse component record for Love waves. To obtain the latter from two horizontal components we use a theoretical backazimuth. The other technique is based on selecting values corresponding to the highest energy of the signal for a given frequency. For strong non-interfering signals, both techniques give very similar results. The presence of large discrepancies indicates low data quality or strong interference.

The main difficulty of any polarization measurement is the interference of two or several signals. FTPAN resolves interfering signals if their group-velocity curves do not cross or pinch. For many continental paths, group velocities of fundamental Rayleigh and Love waves in the range of periods between 30 and 50 s are very close. FTPAN diagrams obtained by processing synthetic seismograms as real records show that strong distortions may occur in this period range if these two waves have comparable amplitudes. The most reliable results for this part of the

spectrum are obtained when, due to the radiation pattern, one of the waves (Rayleigh or Love) is much weaker than the other. Similar conclusions have been reached recently by Pollitz & Hennet (1993). Fortunately, such cases are not at all rare. For the results presented here, Rayleigh waves dominate in the north-north-eastern (NNE) sector (back-azimuths from 25°–45°) and Love waves dominate in the north-east-east (NEE) sector (backazimuths from 50°–96°). To solve this problem in the long run will probably require the generalization of the FTPAN method to incorporate simultaneous waveform fitting for Rayleigh and Love wave parameters.

4 OBSERVATIONS

Table 1 presents the backazimuth measurements for Rayleigh and Love waves at three periods: 60 s, 100 s and 150 s. Because of the nature of the source–receiver geometry in each sector, Rayleigh waves dominate records for events in the NNE sector and Love waves dominate the records for NEE events, so we report only azimuth anomalies for a single wave type in each sector. More detailed backazimuth measurements are shown in Figs 2–5.

4.1 North-north-eastern (NNE) sector

Consider records of surface waves arriving from the NNE sector with backazimuths in the range 25°–45°. The most northern event is in Koryakia (north-eastern Siberia). This event produced a very strong Rayleigh wave at KIV (Fig. 2a) which dominates the seismogram. Waveform complexity is evidence of appreciable scattering and significant Rayleigh wave energy can be seen on the transverse component. On the other hand, at OBN the waveform shown in Fig. 2(b) is much simpler. Rayleigh waves are of larger amplitude than the Love waves, but a clear Love wave is seen on the transverse component. No azimuthal anomalies are visually apparent on the waveforms at OBN. Backazimuth measurements are shown in Fig. 2(c) for both KIV and OBN. We see that for KIV the magnitude of deviation decreases monotonically with period from 17° to practically 0° in the range of periods from 60 to 200 s. The Love wave record is much less regular in this range of periods and estimates of azimuthal deviations can not be performed accurately. For OBN, the measured backazimuth anomalies are uniformly small. The Love wave record at OBN is very spectacular, but no significant azimuthal deviations are found for it either.

The event in the Western Pacific near the southern edge of the Kamchatka Peninsula also produced strong Rayleigh waves at KIV as shown in Fig. 3(a). Again, waveform complexity is diagnostic of scattering with a significant component of Rayleigh wave energy on the transverse component. Fig. 3(b) shows that the OBN waveform is much simpler than the KIV record with no apparent visual evidence of an azimuth anomaly. Fig. 3(c) presents the backazimuth measurements and reveals a strong azimuthal anomaly at KIV with periods around 60 s, but its magnitude decreases with period much more slowly than for the events in Koryakia (Fig. 2c). The anomaly at OBN is much smaller.

The group of events near Urup Island of the Central Kuril

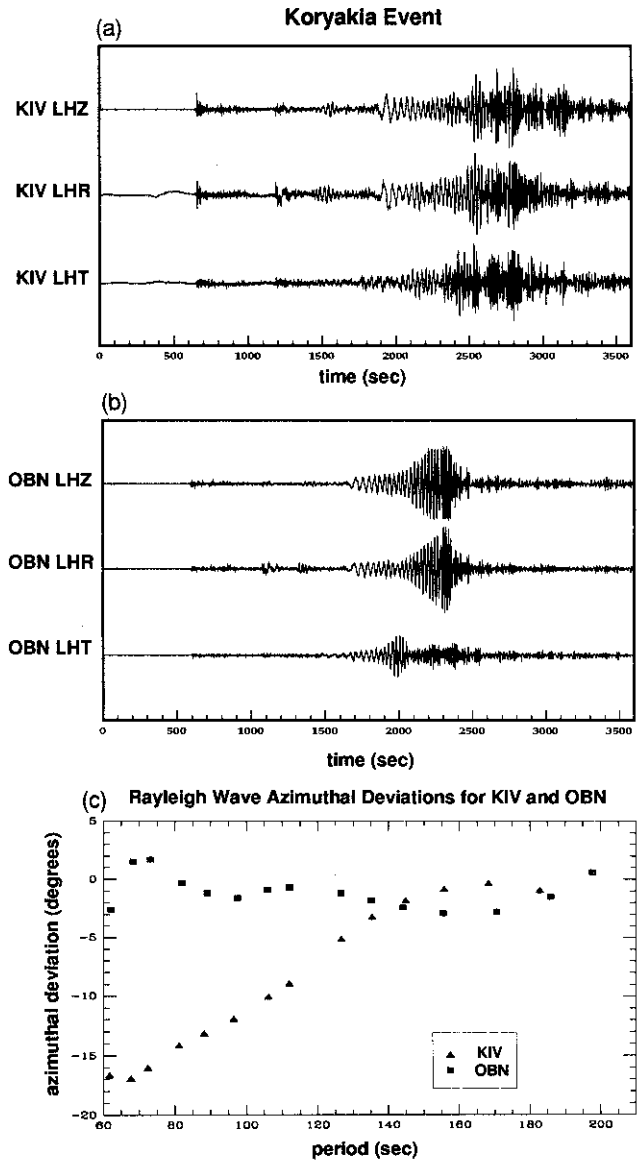

Figure 2. Seismograms for the event in Koryakia, Eastern Siberia, the northernmost event considered, recorded at (a) KIV and (b) OBN rotated into the vertical (top), radial (middle), and transverse (bottom) directions. The KIV record is dominated by Rayleigh waves and waveform complexity is apparent. The OBN record is much simpler, showing little sign of scattering or visually apparent azimuth anomalies. (c) Rayleigh wave azimuthal deviations (in degrees) at KIV and OBN, showing only small anomalies at OBN and a large-magnitude short-period anomaly at KIV. Long-period anomaly is absent for this event at KIV.

Island chain also generated strong Rayleigh waves on records at KIV as can be seen in Table 1. Anomalies observed for the two strongest events are very similar, but very different from those found for the more northerly events, as the Kuril events have a practically constant magnitude of 10°–11° for periods between 100 and 200 s as shown in Fig. 4. For all three events, the sign of deviations is negative, but as the events move south the long-period component of the backazimuth anomalies become larger indicating the emergence of a relatively deep (probably

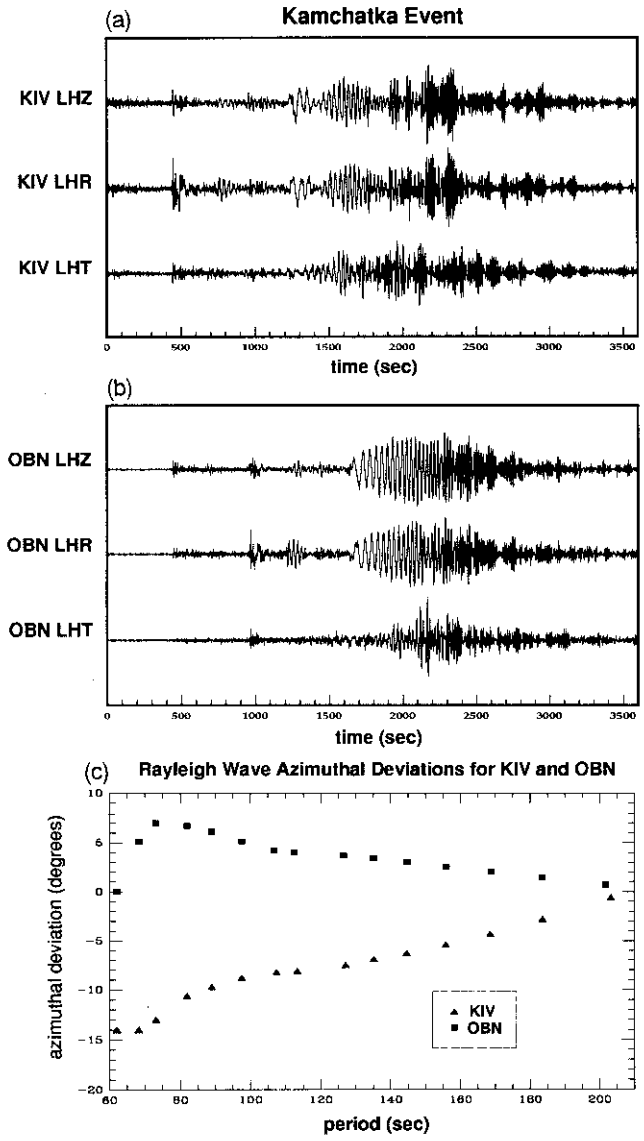

Figure 3. Similar to Fig. 2, but for the Kamchatka event. The long-period anomaly at KIV for this event has developed.

upper mantle) heterogeneity causing the rays to refract more strongly to the north.

4.2 North-east-eastern (NEE) sector

Events near Honshu, the Philippines and Indonesia fall in the range of backazimuths from 50°–96°. Records are dominated by strong fumdamental Love waves with appreciable long-periods energy, as can be seen in Fig. 5(a), and waveforms are complicated, at least at KIV. As can be seen in Table 1, azimuthal deviations are observed through a wide range of periods at KIV but, once again, are relatively small at OBN. The magnitude of the Love wave backazimuth anomalies varies from about 15°–17° at 50–70 s to 10° at 200 s. The event in northern India has a backazimuth close to the Indonesian event, but due to a much smaller epicentral distance to KIV the great circle path is very different. Nevertheless, a strong azimuthal anomaly is found for Love waves in this case. The magnitude and sign of the anomaly are compatible with observations for the Indonesian event. Fig. 5(b) compares the azimuthal deviations at KIV for the events in Honshu, the Phillipines and Sulawesi. Compared to events in the NNE sector, the trends are relatively flat in the period indicating the importance of a deep heterogeneity, and like events in the NNE sector, increase as the paths move southward.

4.3 Reliability of observed path anomalies

Figure 6 demonstrates the repeatability of FTPAN measurements of Rayleigh wave polarization obtained at the station KIV for a cluster of four events near the Kuril Islands. These measurements agree within approximately ±2°. Polarizations measured at KIV from the region around the Kuril Island chain are uniformly about 18° to the north of the great circle linking source and receiver at 75 s period, and trend with period to approximately a constant value of 12° to the north for periods above 100 s. Many examples of repeatability were observed for a variety of source region–station geometries. Errors in instrument magnifications of the order of 5–10 per cent of 3–5° in instrument orientations cannot produce anomalies of the size observed at KIV. If these anomalies are measurement errors, they must come from a major instrument misalignment at KIV. To reject this possibility, it is useful to analyse observations along 'reciprocal' paths. The wave paths from the three Caucasus events on 1991 April 29, 1991 June 15 and 1992 October 23 to MAJO and INU (Honshu, Japan) follow nearly the same path as those from the event of 1990 September 23 near Honshu Island to KIV. Azimuthal anomalies of Rayleigh and Love waves observed at MAJO are of approximately the same magnitude and of the opposite sign as of Love waves observed at KIV, indicating a path deviation to the North (Fig. 7) This confirms that the path anomaly does not result from a major misalignment at KIV. A similar conclusion is reached through analysis of records from the GSN station ANTO (Ankara, Turkey) for western Pacific events, which display similar polarization anomalies to those observed at KIV. The constancy of the long-period polarization anomalies at KIV and MAJO along reciprocal paths means that the source region of the anomaly is neither near KIV nor MAJO.

5 SYNTHETIC EXPERIMENTS

To attempt to illuminate the source region of the polarization anomalies we performed two types of synthetic experiments to address two questions. The first question is whether global-scale models accurately predict the observed polarization anomalies. To address this question, Galerkin ± 5 along-branch coupled normal-mode synthetic seismograms were constructed at periods above 100 s, as described by Resovsky & Ritzwoller (1993), using the global aspherical elastic earth model of Wong (1989). The second question is whether realistic models can be constructed to fit the observed polarization anomalies at KIV. To estimate both the separate and combined effects of regional-scale and global-scale structures along the wave path on surface-wave

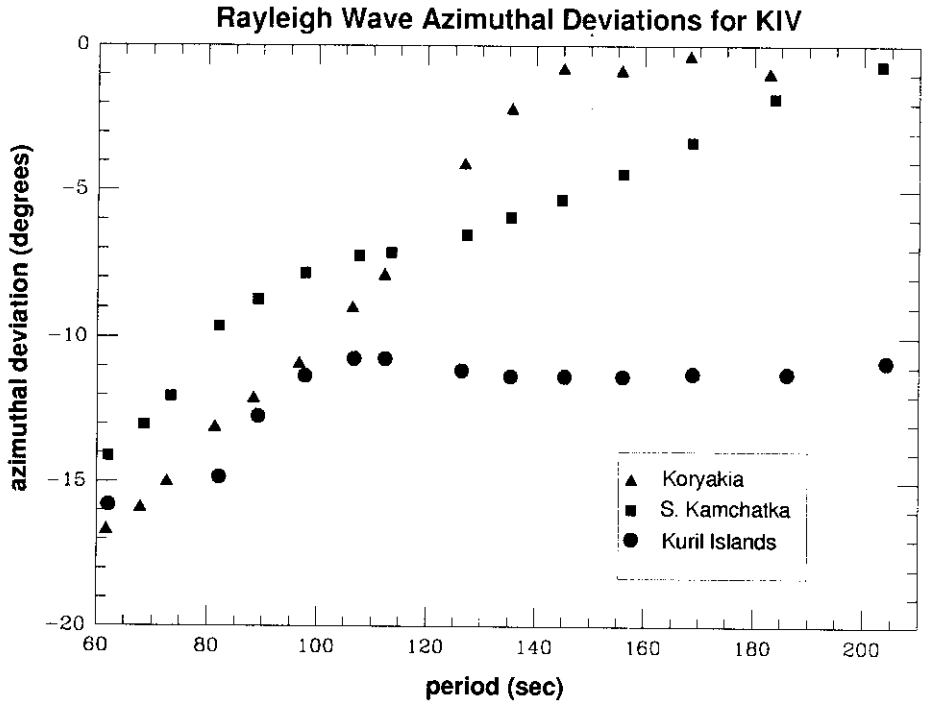

Figure 4 Rayleigh wave azimuthal deviations (in degrees) at KIV for three different events which are, listing from north to south, at Koryakia, Kamchatka, and the Kuril Islands. Azimuthal anomalies are very similar at short periods, but differ at long periods, increasing in magnitude as events move to the south. This is consistent with a lithospheric source region in the neighbourhood of KIV causing the short-period anomalies, and an upper mantle heterogeneity in central Asia causing the long-period anomalies.

polarization we applied the Gaussian-beam summation technique (Červený *et al.* 1982; Yomogida & Aki 1985; Yumogida 1988; Lokshtanov 1990). The code originally developed by Lokshtanov (1990) was significantly modified to account for comparatively sharp horizontal inhomogeneities.

5.1 Long-period synthetic experiments using global-scale aspherical models

Examples of polarization measurements made on the coupled normal-mode synthetic seismograms at KIV and OBN for events at Koryakia, Japan and Indonesia are shown in Fig. 8. These long-period Rayleigh wave synthetic seismograms do not predict such large surface-wave deflections as we observed, at least for R_1. All anomalies at KIV are negative meaning that the paths are moved to the north in agreement with observations for these paths. As the events move southward, the size of the polarization anomaly is increased, also in agreement with observations. Anomalies at OBN are smaller than at KIV for the same events. Therefore, synthetic experiments show that the Eurasian part of the global elastic aspherical model of Wong (1989) ($l \leq 12$) predicts polarization anomalies that are qualitatively but not quantitatively correct. Thus, the global models provide a very useful foundation for surface-wave path studies, but most of the observed polarization anomalies across Eurasia are caused by currently unmodelled upper mantle structures which can be constrained by polarization measurements.

Polarization measurements can also be made on multiply orbiting surface waves. Fig. 9 suggests that these measurements behave in the coupled normal-mode synthetic seismograms in a systematic way, growing in magnitude with orbit as the waves move away from the great-circle path. Such measurements could prove to be useful in the future for constraining global-scale structures as well as regional-scale structures.

5.2 Middle-period synthetic experiments using regional-scale models

The polarization effects of three simple, physically realistic models of lateral heterogeneity (models M1–M3) were studied with the Gaussian-beam synthetic seismogram method (Fig. 10). The model M1 is characterized by smooth lateral changes of crustal thickness and upper mantle velocities in the direction perpendicular to the expected wave path. The horizontal gradient of shear-wave velocity in the upper mantle extending to depths up to 100 km is approximately $2.2 \times 10^{-4}\,s^{-1}$ and half this value for deeper layers. The horizontal gradient of crustal thickness is approximately 2.5×10^{-3}. The values of both gradients are significantly less than those found in regional models of the Central Eurasian lithosphere (e.g. Patton 1980; Pavlenkova & Egorkin 1983; Ryaboy 1989; Beloussov *et al.* 1991). The model M2 has a circular inclusion, simulating a sedimentary basin. Its central point is slightly off the expected wave path and relatively close to the receiver point. The thickness of the sediments decreases with distance from the center of basin; its maximum value is 8 km, which is significantly less than known values of sedimentary thickness in the

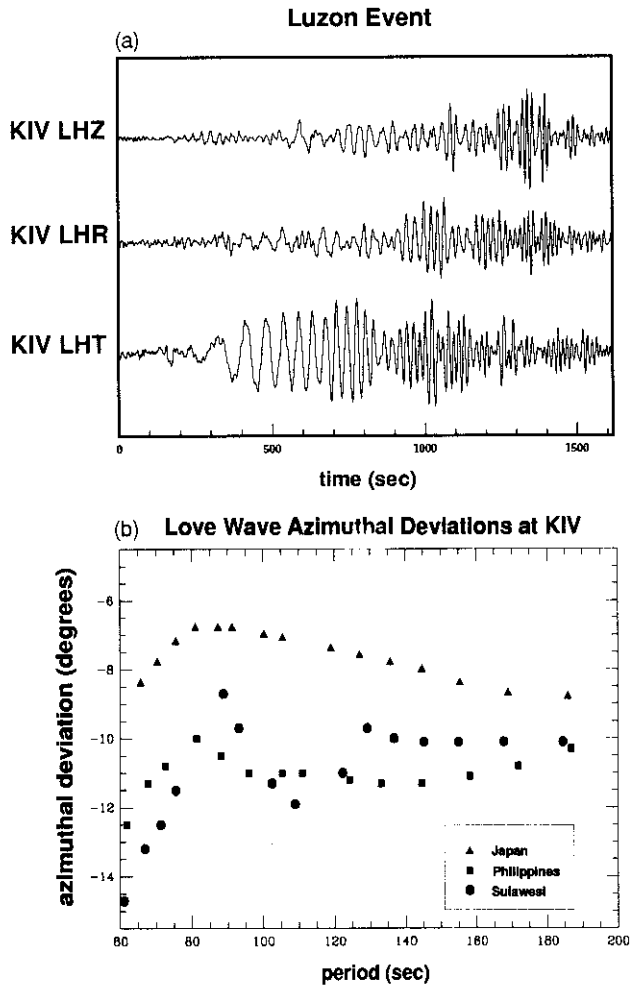

Figure 5. (a) Similar to Fig. 2(a), but for the Panay event. Love waves dominate and waveform complexity is apparent. (b) Same as Fig. 4, but here the azimuthal deviations are for Love waves and the events are at (from north to south): Honshu, Japan; Panay, Philippines; and Sulawesi, Indonesia. The azimuthal deviations are relatively flat in period, indicating an upper mantle heterogeneity in central Asia.

sub-Caspian depression. The medium outside this basin is laterally homogeneous. The model M3 combines both lateral heterogeneities.

Phase velocity maps and ray paths of a fundamental Rayleigh wave for all three models are shown in Fig. 11. Azimuthal deviations as functions of period found by processing synthetic seismograms using the FTPAN technique are shown in Fig. 12. Magnitudes of deviations for the model M1 are of the order 8° for the range of periods between 40 and 250 s. For the model M2 they are above 5° only for periods less than 50 s and disappear for periods longer than 100 s. For the combined model M3, magnitudes of azimuthal deviations decrease from 17° to 10° as period increases from 30 to 100 s and are practically constant for longer periods. Polarization anomalies modelled in such a way are quite similar to the observed anomalies, both in magnitude and frequency dependence. We conclude that two source regions at two scales are necessary to fit the observed polarization anomalies; a regional-scale source to produce the azimuth-dependent short-period anomaly and a much larger scale source to produce the stable long-period anomaly. As discussed in the next section, short-period anomalies undoubtedly result from the waveform effects of the sub-Caspian depression and the long-period anomalies probably result from crustal thinning and increase in upper mantle velocities from south to north across central and northern Asia.

6 DISCUSSION

The magnitude, consistency, and period trends of the observed anomalies of particle motion permit us to consider them to be real phenomena produced by wave propagation effects in the crust and upper mantle, and not merely instrumental or measurement artefacts. The question that remains to be answered is what causes these propagation effects. The wavelengths of the waves under study range from approximately 200 km to more than 1000 km. This provides grounds for rejecting the very local effects of nearby relief and local crustal structure as the main cause of the observed anomalies, at least at long periods.

Anisotropy of the upper mantle material can produce some apparent azimuthal deviations of particle motion from those predicted for isotropic models (Crampin 1975). Anisotropic effects should be mainly due to poloidal–toroidal coupling evidenced as quasi-Rayleigh or quasi-Love energy on unexpected components rather than subtle refractive effects (Park & Yu 1992). However, if local azimuthal anisotropy would play a role in the observed polarization anomaly, one would expect a 180° symmetry in the azimuthal dependence of the anomaly. (M. Cara, private communication, 1993.) No such symmetry is apparent. In addition, to cause anomalies of the observed nature and magnitude we should assume much higher values of anisotropic coefficients than those obtained from tomographic studies of azimuthal surface-wave anisotropy (e.g. Leveque & Cara 1983, 1985). In this study we have intentionally limited ourselves to consider only isotropic models because, as we showed in the previous section, even such simple isotropic models may reproduce anomalies of the observed magnitude.

We interpret the anomalies as the result of lateral 'wandering' of the wave paths due to lateral inhomogeneities of crustal and upper mantle structure. The main inhomogeneities are in high relief regions of Central Asia which makes waves propagating across these structures especially sensitive to such path distortions. We suggest two basic reasons for the observed deviations. One is the presence of significant positive gradients of the phase velocities of surface waves in the direction from south-east to north-west through all of northern and central Eurasia as indicated by the global tomographic models of, for example, Woodhouse & Dziewonski (1984), Tanimoto & Anderson (1985), Smith & Masters (1989), and Wong (1989). This is caused by the thinning of the Earth's crust and the increasing of velocities in the upper mantle (Beloussov *et al.* 1991; Pavlenkova & Egorkin 1983; Ryaboy 1989). Such gradients should produce systematic deviations of ray paths to the north-west, as is observed at KIV. Effects observed at OBN are much smaller due to the more northerly paths of

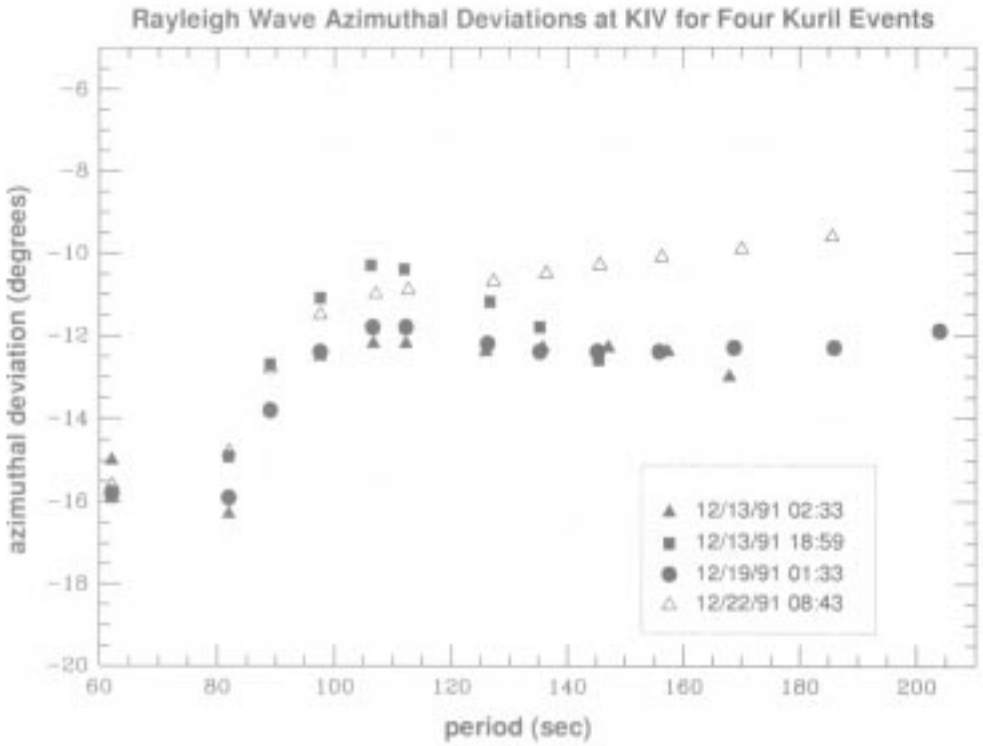

Figure 6. Repeatability of polarization measurements. Rayleigh wave azimuthal deviations observed at KIV for four nearly degenerate events in the Kuril Islands which occurred on 1991 December. Scatter of the deviations is less than 2.5°.

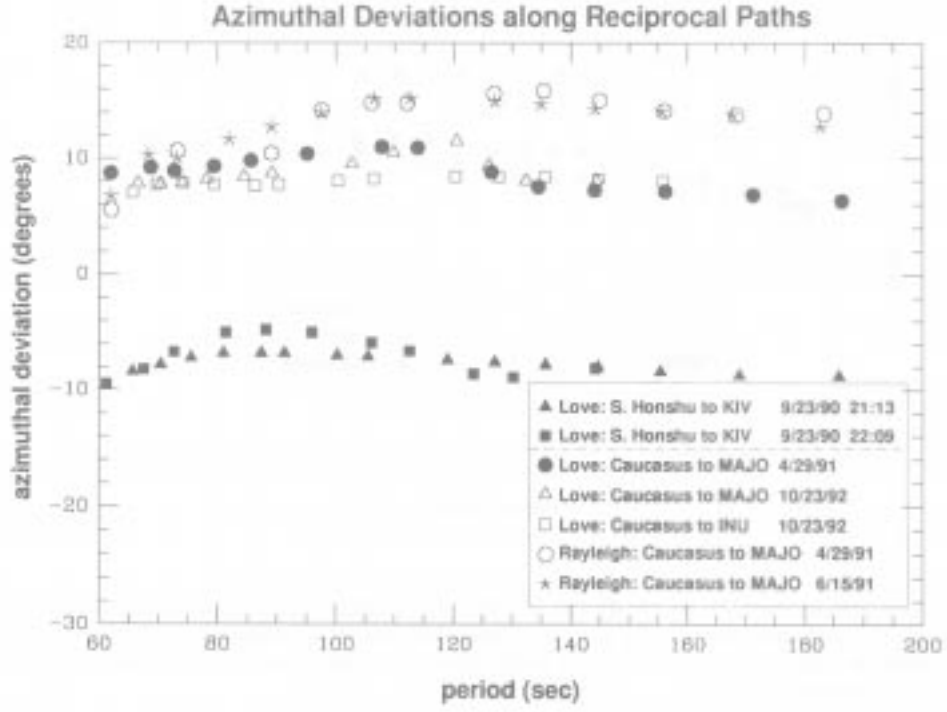

Figure 7. Comparison of azimuthal deviations at KIV, MAJO and INU for 'reciprocal' paths (from two events in S. Honshu with wave paths to KIV for Love waves and from four events in the W. Caucasus to MAJO/INU for Love and Rayleigh waves). The magnitude of the deviations is similar, but their signs are different, indicating for both sets of oppositely travelling waves a deflection to the north.

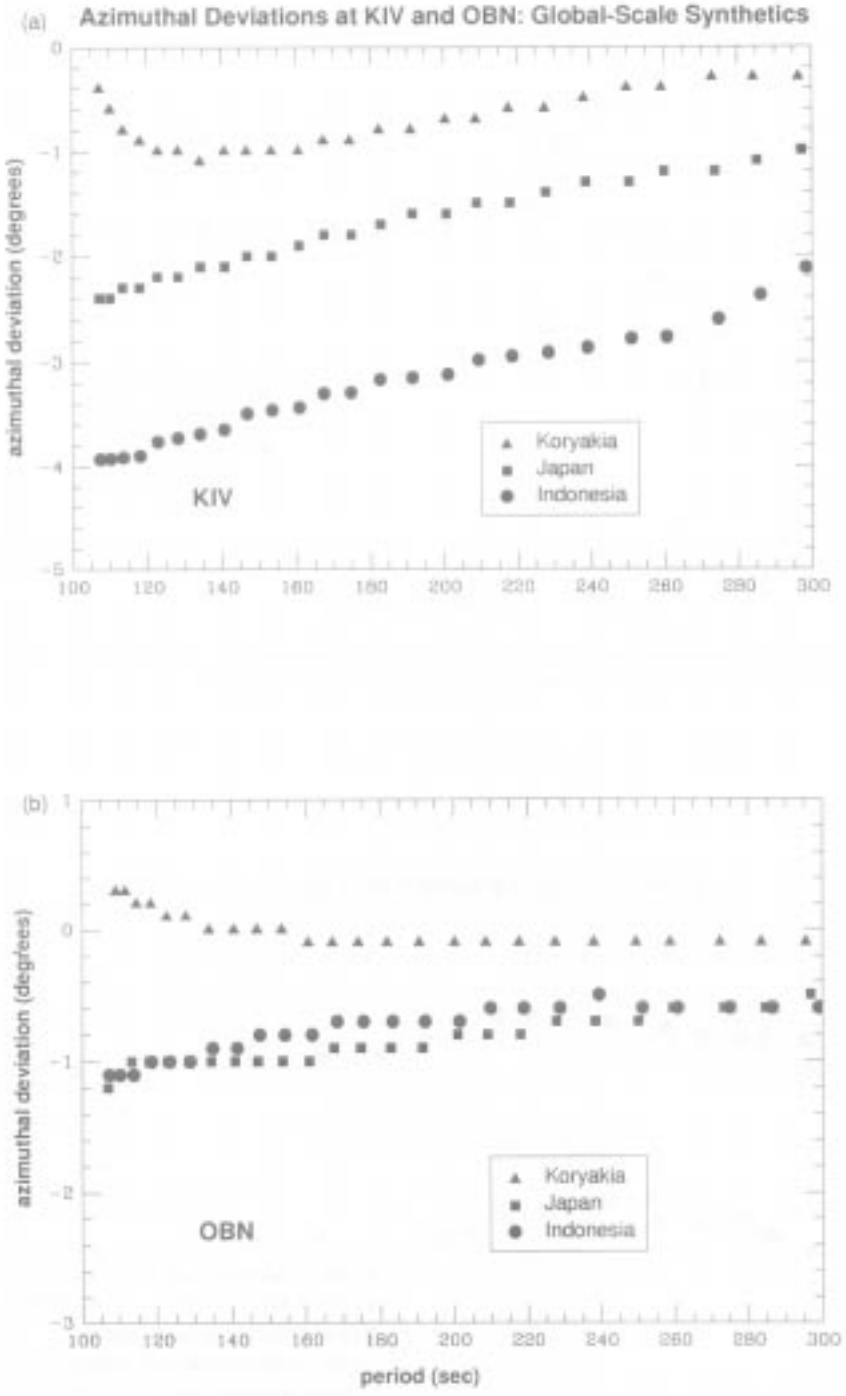

Figure 8. (a) Rayleigh wave polarization anomalies at KIV from long-period coupled normal-mode synthetic seismograms computed with a global-scale aspherical elastic model for three events located in Koryakia, Japan and Indonesia. (b) The same as (a), but for OBN. Long-period synthetics through global-scale aspherical models predict polarization anomalies that are of the right sign, but are too small in magnitude by a factor of approximately five.

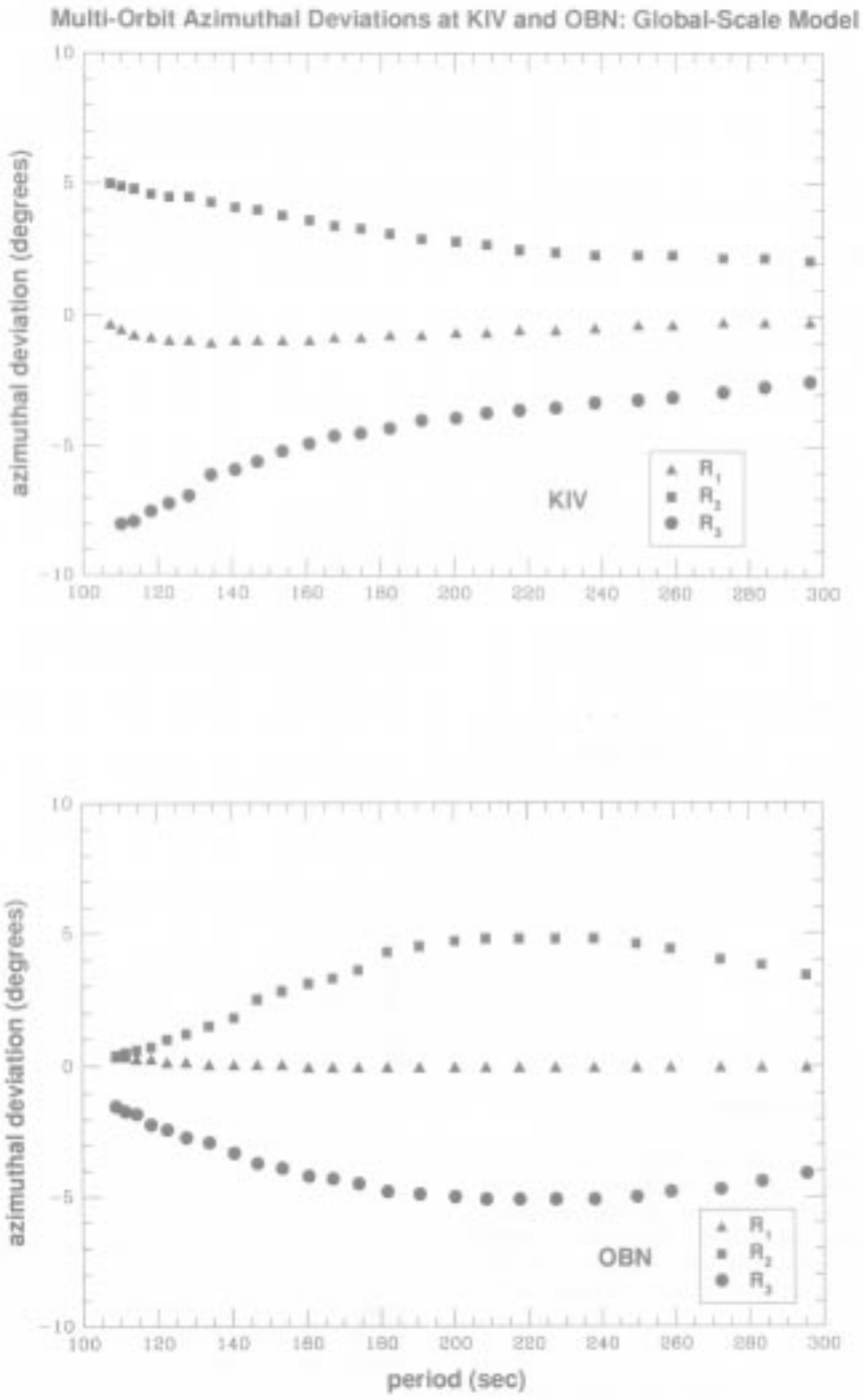

Figure 9. Polarization measurements made on multiply orbiting Rayleigh waves from the normal-mode synthetic seismograms and the global aspherical model indicating the systematic deviation of surface-wave paths from the great circle as a function of orbit number. The moment tensor and event location is the CMT solution for the Koryakia event.

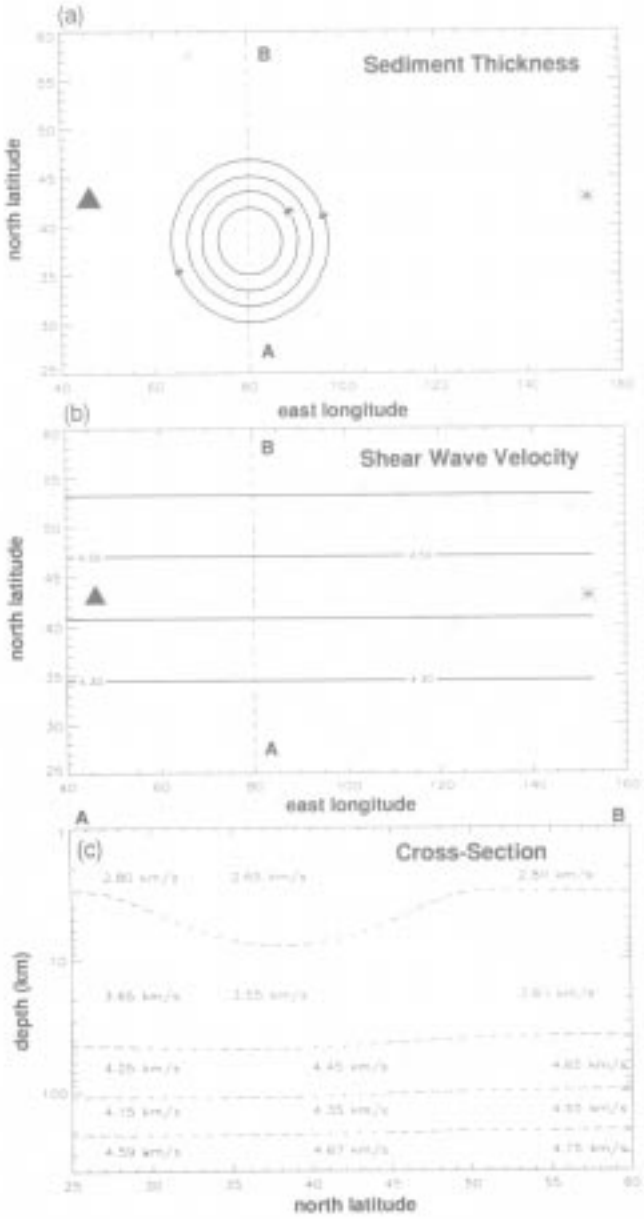

Figure 10. Model M3 used in the Gaussian-beam synthetic experiment. (a) The layer thickness of the 'sedimentary' inclusion, with a maximum thickness of 8 km. (b) Isolines of shear velocities in the lid, grading from lower velocities to the south to higher velocities to the north. (c) Cross-section along the line A–B. The star and the triangle here and below indicate the positions of the source and receiver, respectively.

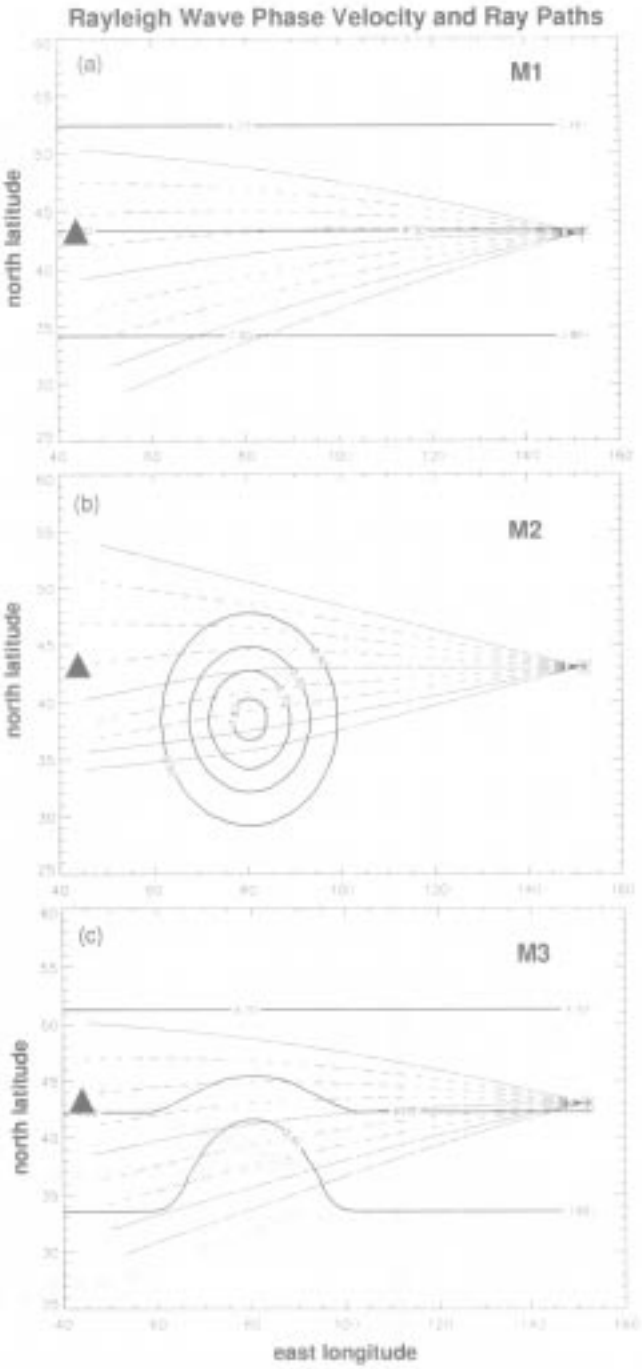

Figure 11. Rayleigh wave phase-velocity maps and rays contributing in the Gaussian-beam summation at the periods $T = 100$ s (models M1, M3) and $T = 40$ s (Model M2).

propagation from the east to this station. It seems that the velocity gradients are smaller in most of northern Eurasia in comparison with the central part of this continent.

The other explanation is based on smaller, regional-scale structures. KIV is surrounded by tectonic zones of distinct origin and history, such as the intracontinental Black and Caspian Seas with a suboceanic crust and upper mantle, the sub-Caspian depression and the Dnepro–Donetski graben with their great thickness of sediments, the mountain ranges of the Caucasus, etc. These structures are comparable to or larger in spatial extent than the wavelengths of the surface waves considered here and may produce some of the observed effects especially at the shorter periods. The slow sub-Caspian depression is directly in the path of waves from NNE, and to avoid it wave paths should significantly deviate to the north. Wave paths from east and south-east may deviate to the north to avoid the main Caucasus range.

Synthetic experiments using long-wavelength global models of lateral heterogeneity do not reveal such large azimuthal anomalies. For fundamental Rayleigh waves

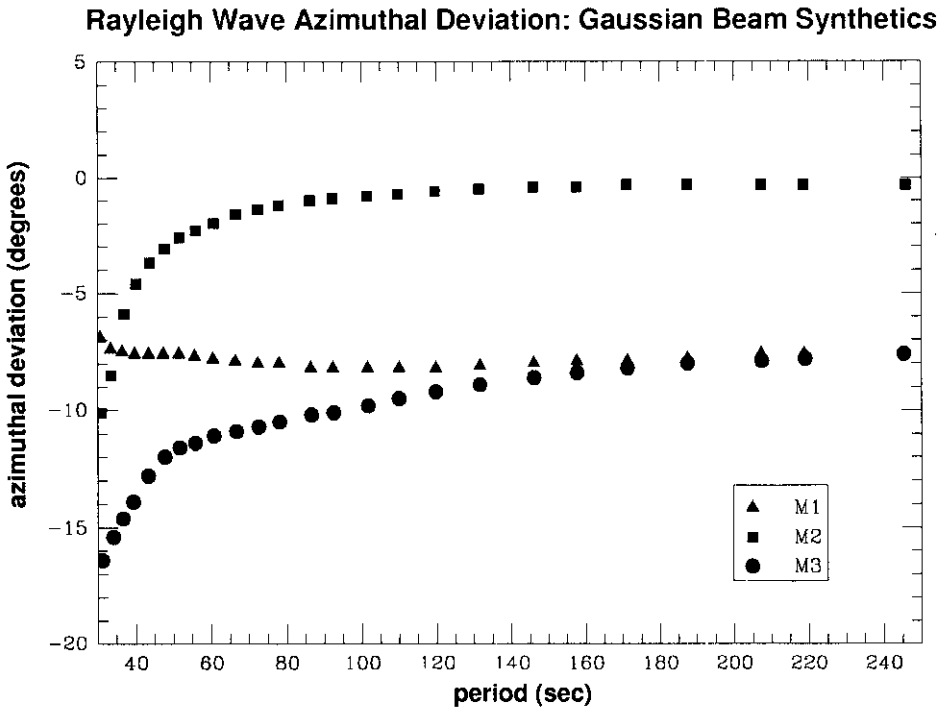

Figure 12. Polarization anomalies for the three models M1–M3 from the Gaussian-beam synthetic seismograms. Predicted anomalies are comparable to those observed for the model M3.

propagating across Eurasia, synthetic azimuth anomalies produced by fundamental-mode along-branch coupling are uniformly less than 5°. Consequently, we conclude that both regional and global scales are essential to produce the observed phenomena. The combination of polarization analyses with array data processing using such networks as are now installed in Kirghizia and in the northern Caucasus may contribute to our understanding in the future.

7 CONCLUSIONS

The FTPAN method produces stable and reproducible polarization measurements for three-component broad-band instruments. Significant particle-motion anomalies have been found on records of surface waves arriving at station KIV from events in the western Pacific. In the period range from 50 to 200 s the magnitude of the azimuthal deviations of particle motion from the great-circle directions varies from 15° to 10°. The most plausible explanation of this phenomenon is the deviation of the ray paths of surface waves from the great circle linking the source and receiver due to large- and intermediate-scale lateral heterogeneities in the Eurasian crust and upper mantle.

To confirm these findings and to attempt to resolve heterogeneities of different scales which potentially produce polarization anomalies, we plan as the next step to perform similar polarization analyses of surface-wave records from all Eurasian broad-band stations of the GSN, CDSN, GEOSCOPE, and IRIS/IDA networks. The ultimate goal will be to use traveltime, amplitude, and polarization information for tomographic inversion of surface-wave data across Eurasia.

ACKNOWLEDGMENTS

We would like to thank M. Cara for a helpful review. In addition, we thank D. Lokshtanov for his Gaussian-beam code, and G. Masters and R. Widmer for their instrument-response subroutines. The authors are grateful to H. Given and S. Ingate at UCSD for their help in obtaining IRIS/IDA recordings obtained in the FSU, to G. Roult for providing the GEOSCOPE records, and to the staff of IRIS's Data Management Center at the University of Washington, in particular T. Ahern and R. Titus, for fulfilling huge data requests.

REFERENCES

Babich, V.M. & Chikhachev, B.A., 1975. Propagation of Love and Rayleigh waves in weakly inhomogeneous media, *Vestnick LGU* **1**, 32–38.

Babich, V.M., Chikhachev, B.A. & Yanovskaya, T.B., 1979. Surface waves in vertically inhomogeneous half-space with weak horizontal inhomogeneity, *Izv. AN SSSR, Fiz. Zemli (Solid Earth)*, **4**, 24–31.

Beloussov, V.V., Pavlenkova, N. I. & Kvyatkovskaya, G. N., (eds), 1991. *Deep structure of the territory of the USSR*, (in Russian), Nauka, Moscow.

Berteussen, K.-A., Levshin, A.L. & Ratnikova, L.I., 1983. Regional studies on the crust in Eurasia with surface waves recorded by the NORSAR group, in *Mathematical Models of the Structure of the Earth and the Earthquake Prediction, Comput. Seism.*, **14**, 106–116.

Bungum, H. & Capon, J., 1974. Coda pattern and multipath propagation of Rayleigh waves at NORSAR, *Phys. Earth planet. Inter.*, **9**, 111–127.

Cara, M. & Leveque, J., 1988. Anisotropy of the asthenosphere:

the higher mode data of the Pacific revisited, *Geophys. Res. Letts.*, **15,** 205–208.

Červený, V., Popov, M. & Pšenčík, I., 1982. Computation of wave fields in inhomogeneous media—Gaussian beam approach, *Geophys. J. R. astr. Soc.*, **70,** 109–128.

Crampin, S., 1975. Distinctive particle motion of surface waves as a diagnostic of anisotropic layering, *Geophys. J.R. astr. Soc.*, **40,** 177–186.

Durek, J.J., Ritzwoller, M.H. & Woodhouse, J.H., 1993. Constraining upper mantle anelasticity using surface wave amplitude anomalies, *Geophys. J. Int.*, **114,** 249–272.

Gee, L. & Jordan, T., 1988. Polarization anisotropy and fine-scale structure of the Eurasian upper mantle, *Geophys. Res. Letts.*, **17,** 993–996.

Given, H., 1990. Variations in broadband seismic noise at IRIS/IDA stations in the USSR with implications for event detection, *Bull. seism. Soc. Am.*, **80,** 1148–1151.

Hu, G. & Menke, W., 1992. Formal inversion of laterally heterogeneous velocity structure from *P*-wave polarization data, *Geophys. J. Int.*, **110,** 63–69.

Lander, A.V. & Levshin, A.L., 1982. Azimuthal and polarization anomalies of surface waves and the methods for studying them, in *Development of G.A. Gamburtsev's Ideas in Geophysics,* (in Russian), pp. 248–260, ed. Galpezin, E. I., Nauka, Moscow.

Lerner-Lam, A.L. & Park, J.J., 1989. Frequency-dependent refraction and multipathing of 10–100 second surface waves in the western Pacific, *Geophys. Res. Lett.*, **16,** 527–530.

Leveque, J. & Cara, M., 1983. Long-period Love wave overtone data in North America and the Pacific Ocean: new evidence for upper mantle anisotropy, *Phys. Earth planet Inter.*, **33,** 164–179.

Leveque, J. & Cara, M., 1985. Inversion of multimode surface wave data; evidence for sublithospheric anisotropy, *Geophys. J. Int.*, **83,** 753–773.

Levshin, A.L., 1985. Effects of lateral inhomogeneities on surface wave amplitude measurements, *Ann. Geophys.*, **3,** 511–518.

Levshin, A.L. & Berteussen, K.-A., 1979. Anomalous propagation of surface waves in the Barents Sea as inferred from NORSAR recordings, *Geophys. J.R. astr. Soc.*, **56,** 97–118.

Levshin, A.L., Ratnikova, L.I. & Berger, J., 1992. Peculiarities of surface wave propagation across the Central Eurasia, *Bull. seism. Soc. Am.*, **82,** 2464–2493.

Levshin, A.L., Yanovskaya, T.B., Lander, A.V., Bukchin, B.G., Barmin, M. P., Ratnikova, L.I. & Its, E.N., 1989. *Seismic surface waves in a laterally inhomogeneous Earth,* (ed. Keilis-Borok, V.I.), Kluwer, Dordrecht.

Lokshtanov, D.E., 1990. Synthetic seismograms computation by Gaussian beams method, *Workshop on Earthquake Sources and Regional Lithospheric Structures from Seismic Wave Data,* Int. Centre Theor. Phys., Trieste.

Montagner, J.-P. & Tanimoto, T., 1990. Global anisotropy in the upper mantle inferred from regionalization of phase velocities, *J. geophys. Res.*, **95,** 4797–4819.

Nataf, J.-C., Nakanishi, I. & Anderson, D.L., 1986. Measurements of mantle wave velocities and inversion for lateral heterogeneities and anisotropy 3. Inversion, *J. geophys. Res.*, **91,** 7261–7307.

Nolet, G., (ed.), 1987. *Seismic tomography,* Kluwer, Dordrecht.

Park, J. & Yu, Y., 1992. Anisotropy and coupled free oscillations: simplified models and surface wave observations, *Geophys. J. Int.*, **110,** 401–420.

Patton, H., 1980. Crust and upper mantle structure of the Eurasian continent from the phase velocity and *Q* of surface waves, *Rev. Geophys. Space Phys.*, **18,** 605–625.

Pavlenkova, N.I. & Egorkin, A.V., 1983. Upper mantle heterogeneity in the northern part of Eurasia, *Phys. Earth. planet. Inter.*, **33,** 180–193.

Paulssen, H., Levshin, A.L., Lauder, A.V. & Snieder, R., 1990. Time- and frequency-dependent polarization analysis: anomalous surface wave observations in Iberia, *Geophys. J. Int.*, **103,** 483–496.

Pollitz, F.F. & Hennet, C.G., 1993. Analysis of Rayleigh wave refraction from three-component seismic spectra, *Geophys. J. Int.*, **113,** 629–650.

Resovsky, J.S. & Ritzwoller, M.H., 1994. Characterizing the long-period seismic effects of long-wavelength elastic and anelastic models, *Geophys. J. Int.*, in press.

Ryaboy, V.Z., 1989. *The upper mantle structure studies by explosion seismology in the USSR,* Delfic Associates, VA.

Smith, M.F. & Masters, G., 1989. Aspherical structure constraints from normal-mode frequency and attenuation measurements, *J. geophys. Res.*, **94,** 1953–1976.

Tanimoto, T. & Anderson, D., 1985. Lateral heterogeneity and anisotropy of the upper mantle: Love and Rayleigh waves 100–200 s, *J. geophys. Res.*, **90,** 1842–1858.

Vidale, J.E., 1986. Complex polarization analysis of particle motion, *Bull. seism. Soc. Am.* **76,** 1393–1405.

Wong, Y.K., 1989. Upper mantle heterogeneity from phase and amplitude data of mantle waves, *PhD thesis,* Harvard University, Cambridge, MA.

Woodhouse, J.H., 1974. Surface waves in a laterally varying layered structure, *Geophys. J.R. astr. Soc.*, **37,** 461–490.

Woodhouse, J.H. & Dziewonski, A.M., 1984. Mapping the upper mantle: Three dimensional modeling of earth structure by inversion of seismic wave forms, *J. geophys. Res.*, **89,** 5953–5986.

Woodhouse, J.H. & Wong, Y.K., 1986. Amplitude, phase and path anomalies of mantle waves, *Geophys. J.R. astr. Soc.*, **87,** 753–773.

Yomogida, K. & Aki, K., 1985. Waveform synthesis of surface waves in a laterally heterogeneous Earth by the Gaussian beam method, *J. geophys. Res.*, **90,** 7665–7688.

Yomogida, K., 1988. Surface waves in weakly heterogeneous media, in *Mathematical Geophysics,* pp. 53–75, eds Vlaar, N.J., Nolet, G., Wortel, M.J.R., & Cloetingh, S.A.P.L., Reidel Publ. Co., Dordrecht.